ARCHIVES OF METALLURGY AND MATERIALS
Volume 51 2006 Issue 1

G. NOLZE*[1)]

INTERPHASE BOUNDARY CHARACTERIZATION IN DUPLEX STEEL AND IRON METEORITES USING EBSD TECHNIQUE

CHARAKTERYSTYKI GRANIC MIĘDZYFAZOWYCH OTRZYMANE TECHNIKĄ EBSD W STALI DUPLEX I W ŻELAZNYCH METEORYTACH

The properties of materials are mainly described by the orientation distribution of the crystalline phases in a material. Beside the so considered anisotropy also the grain as well as phase boundaries are of extreme importance for a whole string of properties, e.g. the strength of a material. On the example of the interface between fcc and bcc iron the discovered and derived models are discussed. Although the common models are based on the crystal lattice description, the atomic configuration on the interface is analysed. Since experimentally a wide spread of orientations data appears the consideration of the frequency distribution is proposed to find at least the main orientation relationship between fcc and bcc. High-indexed pole figures as well as the Euler subspace are introduced in order to increase the accuracy and to compare different measurements. For the sake of simplicity EBSD measurements on iron meteorites are used since they commonly consist of large fcc single crystals which transformed to a low and very specific number of bcc grains. In special cases the described procedure could also be used for steels.

Keywords: orientation relationship, phase boundary, misfit, pole figure, Euler space, variant selection

Opis właściwości materiałów można oprzeć o rozkłady orientacji krystalików różnych faz w przestrzeni próbki. Z rozkładów orientacji można uzyskać informacje o granicach ziarn oraz granicach międzyfazowych, które mają istotny wpływ na szereg właściwości materiału (np. wytrzymałość) Opracowane modele są dyskutowane na przykładzie granic międzyfazowych między żelazem α i γ. Analizowane są konfiguracje atomów w obszarze granicy międzyfazowej. Dla znalezienia głównej zależności krystalograficznej między α i γ analizowano rozkłady częstości orientacji. Aby poprawić dokładność pomiaru, a także, aby móc porównywać wyniki z różnych pomiarów wykorzystywano wysoko-indeksowane figury biegunowe oraz przestrzeń kątów Euler'a. Do badań żelaznych meteorytów, które składają się zwykle z dużych kryształów γ i małej liczby ziarn α, zastosowano pomiary EBSD. Podobna procedura pozostała użyta do badań stali duplex.

1. Introduction

The determination of the phase boundary character in multi-component materials is a very important work since phase boundaries or boundaries in general may influence the properties of materials considerably. In order to evaluate the existing interfaces the misorientation between neighbouring grains can be investigated. For grain boundaries this is usually a comparatively simple procedure since the crystal parameter of the compared grains are identical. In case of two or more phases with dissimilar symmetries it is much more complicated to develop a generally applicable procedure. However, during the last years for two important phase transformations problems this have been discussed several times and continuously improved: the fcc/bcc[2)] and the hcp/bcc[3)] transformation. As the most important metals and alloys pass through this high-low temperature transformation. It has constantly been a recurrent problem since the beginning of metallography. Therefore, it is not surprising that with the development of EBSD this statistically highly relevant technique is used for the explanation of new or the confirmation of already existing models.

Various ideas have been developed in order to describe the orientation relationship (OR) between the fcc (or γ) and the bcc (or α) lattices (see Table 1).

* FEDERAL INSTITUTE FOR MATERIALS RESEARCH AND TESTING UNTER DEN EICHEN 87, 12205 BERLIN, GERMANY

1) invited lecturer

2) fcc: face-centred cubic, bcc: body-centred cubic

3) hcp: hexagonal closed-packed

Nevertheless, in the majority of publications it is distinguished only between Kurdjumov-Sachs[4] (K-S) [1], Nishiyama-Wassermann (N-W) since there the concept of parallel close-packed planes has been utilized. In the last few years Greninger-Trojano (G-T) [3]-[5] became more popular[5], whereas Bain [6] and Pitsch [7] for bcc/fcc interfaces are comparatively rarely discovered. The tendency to apply G-T is not surprising since the experimentally collected data very often showed a deviation from the exact K-S or N-W which is bigger than the accuracy of the applied technique. Numerous transmission electron microscopy (TEM) investigations proved this, e.g. [8], but the statistic of these measurements did not allow a general statement. Here EBSD offers in comparison to TEM an unbeatably fast technique for the evaluation of phase boundaries [9]-[24], although the local resolution in scanning electron microscopy (SEM) is appreciably worse. Therefore one must point out that in principle EBSD is not able to investigate the phase boundary. This can be done only by high resolution TEM. It is rather an investigation of the volume on both sides of the phase boundary under the assumption that the orientation will not change up to the interface.

2. Crystallographic description

The common way to characterize a phase boundary consists in the identification of parallel lattice planes and directions for phase A and phase B, as given in Table 1. One of the reasons is that on this way grain boundaries, i.e. interfaces in single phase materials, have been successfully described. The whole coincident site lattice (CSL) theory is based on this fundamental approach. This is reasonable since the lattice, the crystal parameters and the symmetry of neighbouring grains are identical. In case of phase boundaries this would be an extreme exception. May be, that the lattice type is the same (as for fcc and bcc lattices), perhaps the crystal symmetry[5] as well, but the lattice parameters are usually quiet different. From this follows, that one has to presuppose a lattice misfit on the interface of two different phases. In order to keep up the applied concept of CSL, the near coincident site lattice (NCSL) model has been introduced for two dimensions [25] and later for three dimensions, e.g. [26] and [27]. Also molecular dynamics ([28],[29]) as well as interfacial energy calculations [30] have been carried out in order to find a better approach for a prediction of the phase boundaries as result of phase transformation or precipitation.

The present paper will give a current snapshot what can be done by the use of EBSD, i.e. simply by the measurement of local orientations, in order to characterize the orientation relationship (OR) along the fcc/bcc phase boundary. To this end common tools available in each EBSD software shall be applied: pole figures as well as the Euler space.

3. Comparison of the models

The crystallographic description of the individual models in Table 1 suggests a quiet different arrangement of grains so that the interphase interfaces should show clear differences. However, if one analyses the arrangement of the unit cells for fcc and bcc – cf. Fig. 1, it becomes obvious, that the models are very close to each other in spite of their extremely different crystallographic description. They only show a small but distinctly different tilt against each other but the position of the dark-grey bcc cube is in general very similar. This is amazing since it assumes that the atomic movements during transformation are not so different from the expected, because they are fixed by the lattice description. Moreover, the apparent 45° rotations of both cubes in Fig. 1 are again caused by the crystallographic redefinition of the same atomic arrangement, firstly described as face-centred lattice and secondly as body-centred lattice. The necessary lattice distortions which are required to transform an fcc in a bcc lattice are the reason for the visible tilt angles which are assumed in the respective models.

TABLE 1
Overview about the most-frequently referred orientation relationship models in order to describe fcc/bcc interfaces. To this end parallel lattice planes and lattice directions are used

Orientation relationship	plane	direction
Bain	$\{001\}_{fcc} \parallel \{001\}_{bcc}$	$\langle 010\rangle_{fcc} \parallel \langle 110\rangle_{bcc}$
K-S	$\{111\}_{fcc} \parallel \{110\}_{bcc}$	$\langle 1\bar{1}0\rangle_{fcc} \parallel \langle 1\bar{1}1\rangle_{bcc}$
N-W	$\{111\}_{fcc} \parallel \{110\}_{bcc}$	$\langle 0\bar{1}1\rangle_{fcc} \parallel \langle 001\rangle_{bcc}$
G-T	$\{111\}_{fcc}$ $\bar{1}°$ to $\{110\}_{bcc}$	$\langle \bar{1}2\bar{1}\rangle_{fcc}$ $\bar{2}°$ to $\langle 1\bar{1}0\rangle_{bcc}$
Pitsch	$\{100\}_{fcc} \parallel \{1\bar{1}0\}_{bcc}$	$\langle 011\rangle_{fcc} \parallel \langle 111\rangle_{bcc}$

Therefore one can follow that the atomic movements during phase transformation from fcc to bcc are at first not very big, and at second comparatively similar. However, for the model-specific interface planes the appearance of the atomic layers must be different, if they are related to completely different planar symmetries – see Fig. 2. So for B a i n and P i t s c h a four-fold symme-

[4] From the point of view of some scientists, actually Young [2] is the first discoverer of the K-S model, so that they propose to call it Y-K-S model.

[5] for bcc and fcc the point-group symmetry is identically but the space-group symmetry it is not

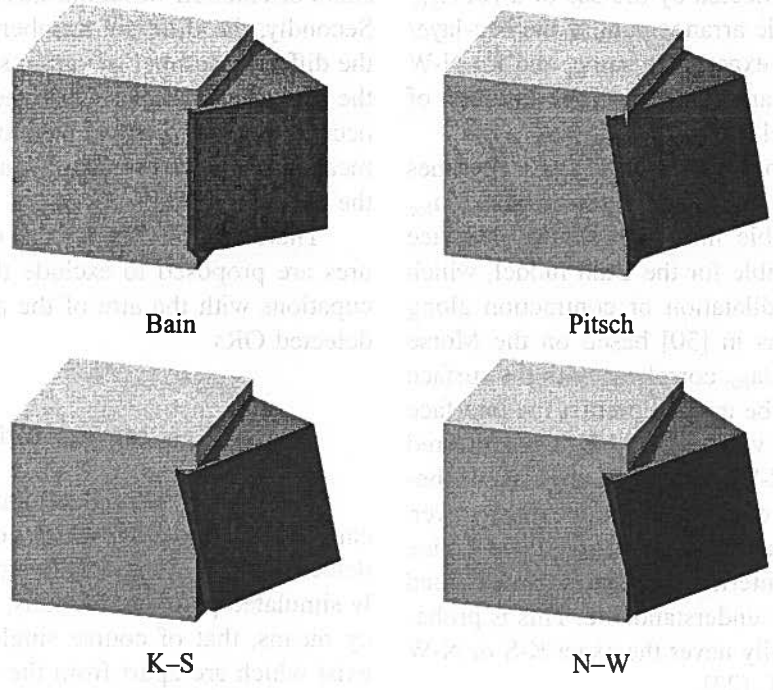

Fig. 1. Intersection of the fcc unit cell (light-grey) and the bcc unit cell (dark-grey) for different OR models

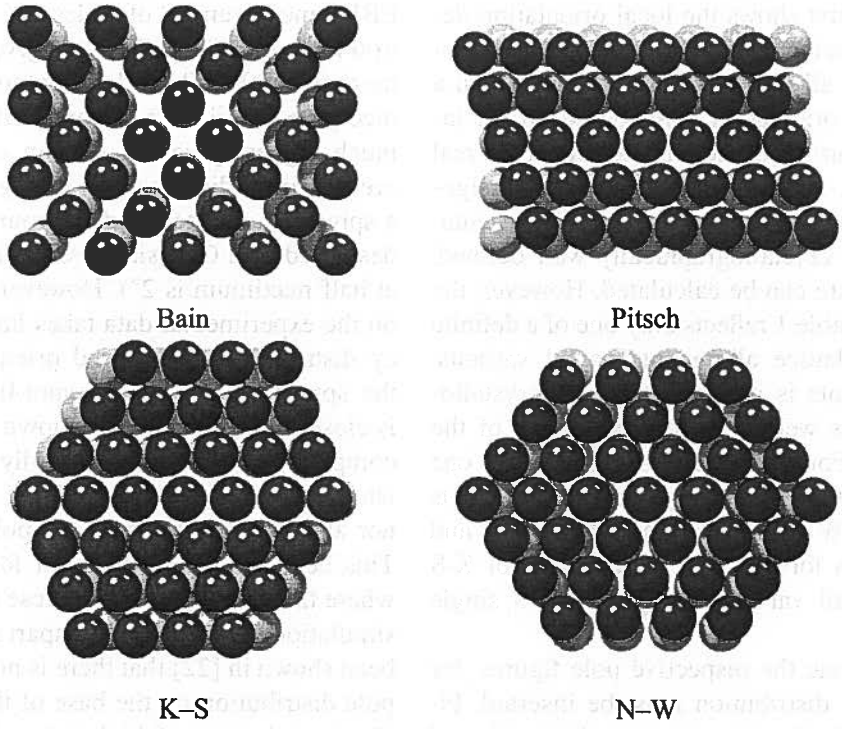

Fig. 2. Schematic interfaces between an fcc layer (light-grey) and an bcc layer (dark-grey), given for the models in Fig. 1. Despite the very similar lattice arrangement the atomic configurations on the interface are quiet different

try of the fcc plane is used whereas for K-S and N-W a three-fold symmetry is reflected by the use of a $\{111\}_{fcc}$ – plane. The planar atomic arrangement of the bcc-layer is for Pitsch and K-S exactly the same, and for N-W only rotated by – 54.74° around the normal direction of the layer which is parallel to the $\{011\}_{bcc}$.

If one looks at the atomic layers in Fig. 2 it becomes obvious that the ratio of the lattice parameters a_{bcc}/a_{fcc} should have a considerable influence on the interface misfit. This is clearly visible for the Bain model, which only describes a lattice dilatation or contraction along the interface. Calculations in [30] based on the Morse potential showed that a_{bcc}/a_{fcc} correlates with the surface energy and can therefore be used to predict the interface characteristic. Close to a value of 0.92 K-S is preferred whereas close to 1.06 N-W preferably appears. In between these values, both of them may appear. However, a element segregation may shift the ratio of the lattice parameters so that such intermediate states as described in the G-T model become understandable. This is probably the reason why virtually never the exact K-S or N-W model has been found, cf. [23].

4. Pole figure representation

The representation of orientation measurements collected with EBSD is usually done by orientation maps or pole figures. The first shows the local orientation description of a sample reference direction, the second represents the totality of all orientation measurements in a pole figure. Whereas orientation maps based on the inverse pole figure colouring are not able to reflect the real orientations detected, in pole figures the local assignment of the measurements are "lost". Since the orientation relationships are crystallographically well defined, the resulting pole figure can be calculated. However, the given description in Table 1 reflects only one of a definite number of possible lattice alignments called variants. The number of variants is dependent on the crystallographic description as well as on the symmetry of the participated crystals. For the models listed in Table 1 one derives 3 independent but symmetry-equivalent variants for Bain, 12 for N-W and Pitsch respectively, and 24 for K-S as well as for G-T. On the example of K-S and N-W in Fig. 3 all variants are given for a single $\{111\}_{fcc}$ plane.

In order to generate the respective pole figures, for each variant the pole distribution must be inserted. Finally, the required pole figures are a superimposition of 3, 12 or 24 single pole figures. Commonly standard pole figures as in Fig. 4 are published. They show several specifics. First of all the occupation of poles in the same region of the pole figure are remarkable, but on the other hand this must be expected since by the use of Fig. 1 the small orientation variations has been already pointed out. Secondly, the different number of poles are a result of the different number of variants for each model. Thirdly, the blackness of dots reflects the number of hidden poles occupying the respective position in the pole figure, what means that multiple occupations exist in dependence on the existing model.

Therefore, in [31] the use of high-indexed pole figures are proposed to exclude the effect of multiple occupations with the aim of the accuracy improvement of detected ORs.

5. A representative example

The use of pole figures has the advantage, that one can define a main OR which considers the frequency of detected orientations only by comparison with previously simulated pole distributions. Considering the frequency means, that of course single orientation events may exist which are apart from the expected main positions, but the number of these orientations are comparatively small so that they show no or only a small effect in the convoluted pole figure and therefore on the main OR. The main OR is presently defined as the most important influence of phase boundaries on the macroscopic property of a material. As example the orientation data of a EBSD measurement of a plessitic region in the Agpalilik iron meteorite (Cape York) is given in Fig. 5. It contains more than 200000 single orientation measurements. The nice pole distribution is remarkable although there is a much bigger spread of data in comparison to the theoretical pole distributions in Fig. 4 which considering a spread of orientation data around the ideal orientation described by a Gaussian distribution function (full width at half maximum is 2°). However, a convolution applied on the experimental data takes into account the frequency distribution of detected orientations and transforms the spread of data into a spot-like arrangement which is close to the simulations shown above. A more precise comparison of the experimentally detected and the simulated pole arrangements in Fig. 4 shows that neither K-S nor all other models fulfil the pole distributions exactly. This becomes especially clear for the {111}-pole figure where the outer spots come close together whereas in the simulation they are further apart from each other. It has been shown in [22] that there is no chance to describe the pole distribution on the base of the derived OR models. The introduction of high-indexed lattice plains and directions as described in [32] in order to be able to define small deviations from these models are comparatively inconvenient. Additionally, the required use of integers for {hkl} and ⟨uvw⟩ limits the accuracy of this description.

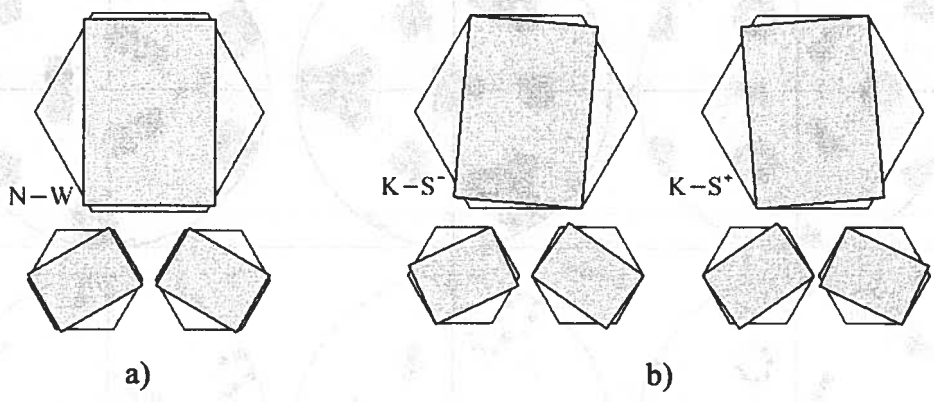

Fig. 3. Possible arrangements of $\{001\}_{bcc}$ planes (dark-grey) on a single $\{111\}_{fcc}$ plane (light-grey). For N-W (a) three equivalent alignments are possible, for K-S (b) even six exist. Since four independent {111}fcc planes exist the final number results after quadruplication of a) and b)

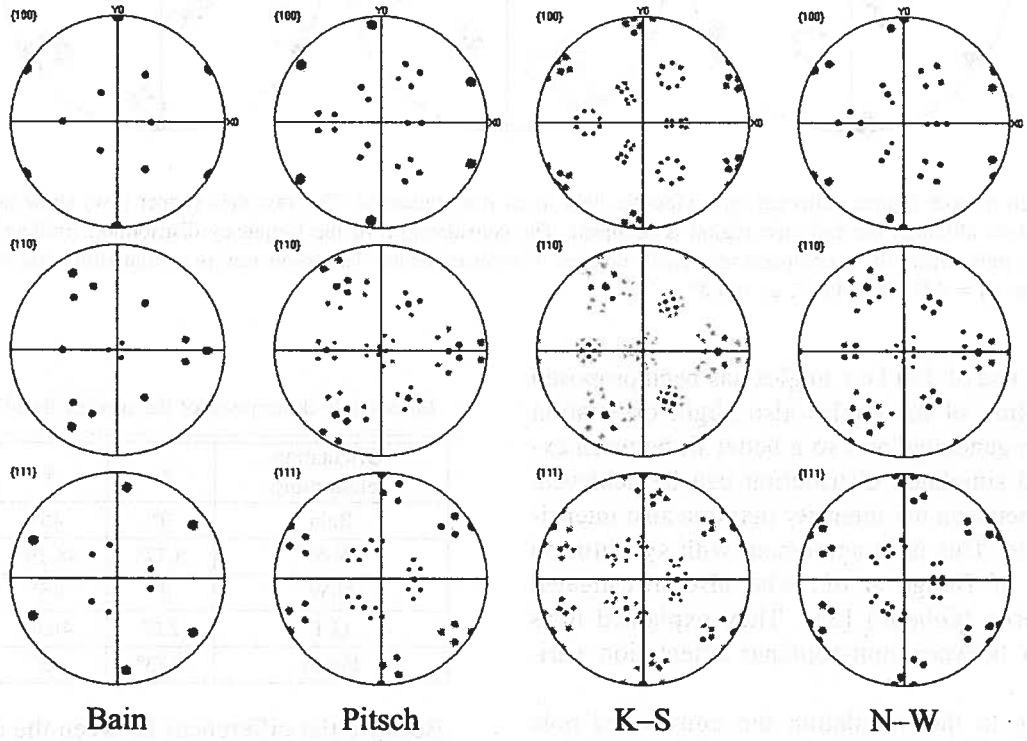

Fig. 4. Simulations of standard pole figures for different OR models. It is obvious that despite the similar pole distribution for Pitsch, K-S and N-W the characteristic of pole alignments allows to distinguish between them

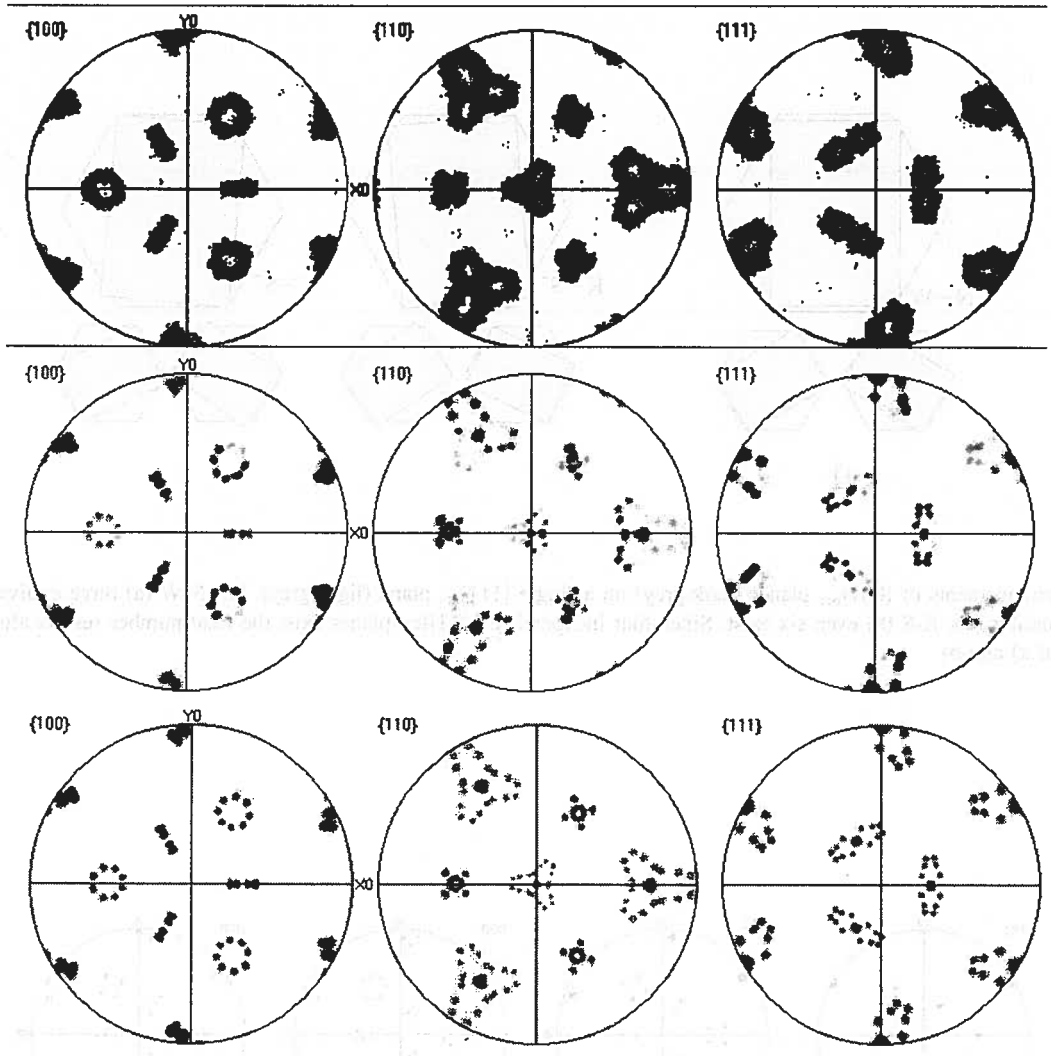

Fig. 5. Comparison of pole figures collected on a plessitic field in an iron meteorite. The raw data (upper row) show an amazingly wide spread of orientations although the expected region is occupied. The consideration of the frequency distribution (middle row) reflects that the wide spread is only caused by a comparatively small number of measurements. The lower row is a simulation describing the OR by a set of Euler angles: $\varphi_1 = 4.8°$, $\Psi = 46.1°$; $\varphi_2 = 4.8°$

To this aim the use of E u l e r angles has been proposed [22]. By variation of the angles also slight orientation changes can be generated and so a better fit between experimental and simulated distribution can be achieved. Nevertheless, between the intensity maxima also intensity is still visible. This is in agreement with synchrotron measurements of Bunge *et al.*, who also investigated an iron meteorite (Gibeon) [33]. They explained it as transition path between non-coplanar orientation variants.

Comparing to the simulation the convoluted pole figures appears not so homogeneous in the blackness of the spots. This is related to the variant selection. If a variant is not or rarely chosen during transformation, e.g. caused by an accumulated stress field, it will appear in the pole figure with a lower blackness.

TABLE 2
Euler angle description of the models listed in Table 1

Orientation relationship	φ_1	ψ	φ_2
Bain	0°	45°	0°
K-S	5.77°	48.19°	5.77°
N-W	0°	45°	9.73°
G-T	2.6°	46.6°	7.5°
Pitsch	9.73°	45°	0°

Because the differences between the defined models are so small the used Euler space can be reduced to a very small subspace which contains at least one representative variant of each model. One set of variants is given in Table 2. The respective representation in a

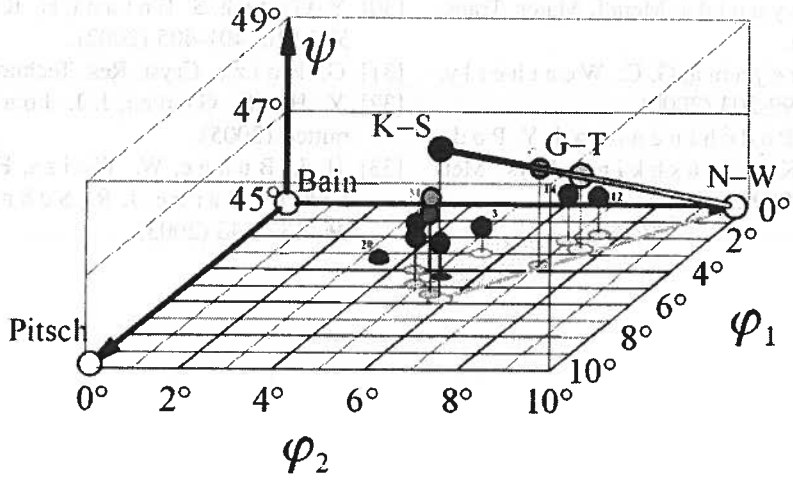

Fig. 6. The Euler-subspace describes the main models (big circles) as well as all experimentally detected OR in steel and meteorites (small circle). Approximately in the middle of the path between N-W and K-S the model of G-T is described

cartesian coordinate system is shown in Fig. 6. There are beside of the models (big circles) a whole string of measurements are given as small circles. Until now we only found some micro-structures in steel or in iron meteorites which show an agreement with the G-T model. Representatives for the other models could not been detected. It is rather so that the main ORs are better described by an intermediate state of all models.

Acknowledgements

This work was partly supported by the Deutsche Forschungsgemeinschaft (GE-497/4-1) and the DAAD. It is based on a fruitful collaboration between the Federal Institute for Materials Research and Testing, the University of Leipzig, and the Warsaw University of Technology. The author would like to thank S. Brookes for reviewing the manuscript and A. Epishin for the numerous discussins.

REFERENCES

[1] G. Kurdjumov, G. Sachs, Z. Phys. **64**, 325-343 (1930).
[2] J. Young, Proc. Royal Soc. Lond. A **112**, 630-641 (1926).
[3] Z. Nishiyama, Sci. Rep. Tohoku Imp. Univ. Tokio **23**, 637-664 (1934).
[4] G. Wassermann, Mitt. K.-Wilh.-Inst. Eisenforsch. **17**, 149-155 (1935).
[5] A. B. Greninger, A. R. Troiano, Met. Trans. **185**, 590-598 (1949).
[6] E. C. Bain, N. Y. Dunkirk, Trans. AIME **70**, 25-46 (1924).
[7] W. Pitsch, Arch. Eisenhüttenw. **38**, 853-864 (1967).
[8] C. H. Shek, C. Dong, J. K. L. Lai, K. W. Wong, Metall. Mat. Trans. **31A**, 15-19 (2000).
[9] A. F. Gourgues, H. M. Flower, T. C. Lindley, Sci. Technol. **16**, 26-40 (2000).
[10] G. Brückner, J. Pospiech, I. Seidl, G. Gottstein, Scripta mater. **44**, 2635-2640 (2001).
[11] M. Ueda, H. Y. Yasuda, Y. Umakoshi, Acta mater. **49**, 4251-4258 (2001).
[12] B. Verlinden, P. Bocher, E. Girault, E. Aernoudt, Scripta mater. **45**, 909-916 (2001).
[13] D.-W. Suh, J.-H. Kang, K. H. Oh, H. C. Lee, **46**, 375-378 (2002).
[14] S. Morito, H. Tanaka, R. Konishi, T. Furuhara, T. Maki, Acta mater. **51**, 1789-1799 (2003).
[15] B. Gardiola, C. Esling, M. Humbert, K.-E. Hensger, Adv. Engin. Mater. **5**, 283-287 (2003).
[16] M. G. Glavicic, P. A. Kobryn, T. R. Bieler, S. L. Semiatin, Mater. Sci. Engin. 346, 50-59 (2003).
[17] N. Gey, M. Humbert, J. Mater, Sci. **38**, 1289-1294 (2003).
[18] G. Nolze, V. Geist, Cryst. Res. Technol. **39**, 343-352 (2004).
[19] A. Lambert-Perlade, A. F. Gourgues, A. Pineau, Acta mater. **52**, 2337-2348 (2004).
[20] S. Zaefferer, J. Ohlert, W. Bleck, Acta mater. **52**, 2765-2778 (2004).
[21] M. Ferry, W. Xu, Mater. Charact. **53**, 43-49 (2004).
[22] G. Nolze, Z. Metallk. **95**, 744-755 (2004).
[23] Y. He, S. Godet, J. J. Jonas, Solid State Phenom. **105**, 121-126 (2005).
[24] H. Kitahara, R. Ueji, M. Ueda, N. Tsuji, Y. Minamino, Mater. Character. **54**, 378-386 (2005).

[25] M. G. Hall, H. I. Aaronson, K. R. Kinsman, Surf. Sci. **31**, 257- 274 (1972).
[26] Q. Liang, W. T. Reynolds, Metall. Mater. Trans. **29A**, 2059-2072 (1998).
[27] N. Miyano, K. Ameyama, G. C. Weatherly, ISIJ International **40**, 199-203 (2000).
[28] V. A. Teplov, G. L. Podchinenova, I. Y. Podchinenov, T. K. Kondrashkina, Phys. Met. Metallogr. **68**, 18-26 (1989).
[29] K. Kadau, R. Meyer, P. Entel, Surf. Rev. Lett. **6**, 35-43 (1999).
[30] Y. Gotoh, S. Entani, H. Kawanowa, Surf. Sci., 507-510, 401-405 (2002).
[31] G. Nolze, Cryst. Res. Technol. in press (2005).
[32] Y. He, S. Godet, J. J. Jonas, J. Appl. Cryst. submitted (2005).
[33] H. J. Bunge, W. Weiss, H. Klein, L. Wcislak, U. Garbe, J. R. Schneider, J. Appl. Cryst. **36**, 137-140 (2003).

Received: 5 January 2006.